Rapid Communication

Cooperative enhancement of fungal repelling performance by surface photografting of stereochemical bi-molecules

Chen Chen, Zixu Xie, Pengfei Zhang, Yanhui Liu, Xing Wang [*]

Beijing Laboratory of Biomedical Materials, Beijing University of Chemical Technology, Beijing 100029, PR China

ARTICLE INFO

ABSTRACT

Fungal contamination could increase exponentially on any convenient sites if without antifungal agents, thus seriously threatening human health. In this work, a cooperative fungal repelling coating has been fabricated by surface photografting polymerization of bi-molecules, polyethylene glycol diacrylate (PEGDA) and bornyl acrylate (BA), which combined amphiphilic feature with stereochemical fungal repelling strategy. ATR-FTIR and EDS were used to confirm the synthesized copolymers. The surface microstructures of the coating film were showed with AFM and SEM images. The cooperative enhancement of fungal repelling performance has been demonstrated through modulating the ratio between hydrophilic PEGDA and hydrophobic BA. When the ratio of monomers was 1:1, the coating exhibited the best cooperative effect on anti-adhesion of *Aspergillus niger*. Binary cooperation between PEG ring and bornyl cage is considered to play a crucial role in this coating system. Therefore, amphiphilic-stereochemistry is believed to be an effective strategy to prevent fungal adhesion.

1. Introduction

Microorganisms (such as bacteria, fungi, etc.) adhere to the surface of materials and form biofilms that may cause related infections and even human death [1]. Thus, preventing harmful microorganisms from contaminating the material surface has become a research hotspot in the fields of biomedicine and food storage [2,3], especially under COVID-19 pandemic conditions. A number of methods have been developed to prevent microbial adhesion [4–6], such as non-release coating based on polyethylene glycol (PEG) [7], zwitterions [8], etc. and release coating based on metal ions [9], antibiotics [10], etc. Most of these reports have demonstrated the effectiveness of either individual or synergistic antimicrobial adhesion methods against bacteria, but only few have been associated with resistance to fungal adhesion. Fungi can adhere to the surface of most materials and spread spores, posing a serious threat to human health [11]. Therefore, it is of great significance to develop new fungal repelling surface.

In recent years, a series of borneol-based polymers have shown antiadhesion and anti-biofilm formation effects on bacteria and fungi [12–14]. By grafting borneol to the surface of graphene [15] and textiles [16], anti-adhesive effects against bacteria and fungi were also achieved. It is believed that these unique antimicrobial adhesion properties are caused by the complex stereochemical structure of borneol

molecules. However, when we tried the surface photografting polymerization [17–19], which can modify various inert polymers surface only containing C—H, we found that bornyl acrylate (BA) monomers couldn't achieve the ideal fungal repelling effect.

We have also noticed that PEG and its derivatives are widely used in the surface modification of biomedical materials to prevent protein and microorganism adhesion [20], but their resistance to fungal adhesion is insufficient [21–24], in particular on linear PEG modified surface. Maybe it is because most fungi like wet environments [25,26], and the surface of PEG just provides hygroscopicity or a wetting property [27].

Herein, a new surface-photografting method combining the two molecules of hydrophobic BA and hydrophilic PEGDA was proposed. Both of them contain distinct stereochemical characteristics of borneol cage and glycols coil. By optimizing the ratio of hydrophilic coil to hydrophobic cage, the synergistic effect of both film-forming and fungal repelling properties can be achieved under the unique bimolecular cooperation. To our knowledge, this is the first time to improve fungal repelling properties based on the amphiphilic stereochemical strategy.

---

* Corresponding author.
E-mail address: wangxing@mail.buct.edu.cn (X. Wang).
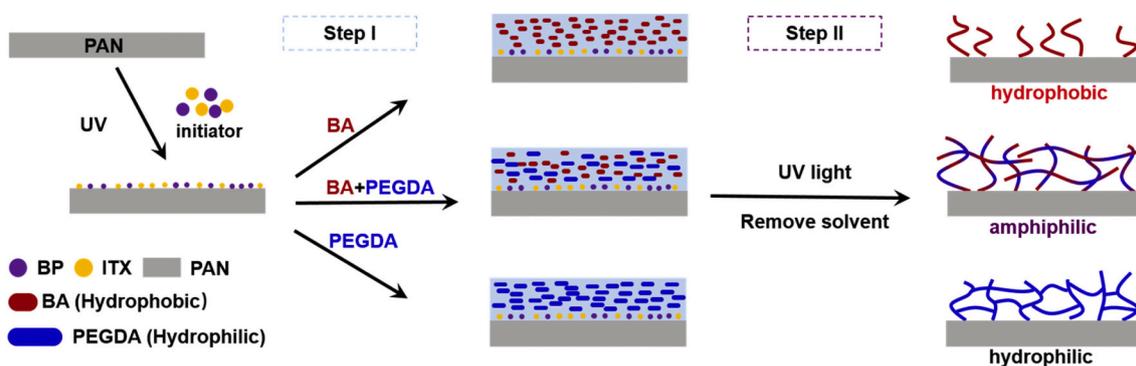
Scheme 1. Process of surface photografting. UV light was used to initiate polymerization and grafting of BA and PEGDA monomers onto PAN surface in two steps.

2. Experiment

2.1. Materials

Isopropyl thioxanthone (ITX) and isobornyl acrylate (BA, 98%) were purchased from J&K Scientific. Polyethylene glycol diacrylate (PEGDA, Mn ~ 200) was purchased from Meryer (Shanghai) Chemical Technology Co., Ltd. Benzophenone (BP) was purchased from Fuchen Chemical Reagent Co., Ltd. Acetone, dichloromethane, ethanol dimethylformamide (DMF) were purchased from Beijing Chemical Plant. Polyacrylonitrile (PAN) powder was purchased from Zhengzhou Alpha Chemical Co., Ltd. *Aspergillus niger* (*A. niger*, ATCC 16404) was purchased from China Centre of Industrial Culture Collection. Malt Extract Agar was purchased from Beijing Aoboxing Biotechnology Co., Ltd.

2.2. Preparation of PAN films

PAN powder (10 g) was first dissolved in 60 mL DMF, then placed in an incubator at 210 rpm, 60 °C for 24 h. After completion, it was put into a vacuum box at 60 °C to get rid of the bubbles. PAN films were prepared by automatic coating machine. Briefly, PAN powder solution was poured over the Non-woven and then set the thickness to 200 μm to complete the coating process. Finally, the films were immersed in deionized water for 24 h with a change of water every 12 h to complete the phase inversion process.

2.3. Surface photografting of PAN films and characterization

PAN films were cut into 8 cm × 8 cm squares. The process of surface photografting is shown in Scheme 1. As previously described [28], the process is performed in two steps. PAN was first modified with BP and ITX. Briefly, a predetermined amount of ITX and BP acetone solution (80 μL, 0.3 g·mL^{-1}) was coated onto the PAN film and then spread into a very thin liquid layer by a quartz plate (10 cm × 10 cm), thus giving rise to a reaction model. The model was irradiated for 8 min at room temperature under a 1000 W high-pressure mercury lamp (Light intensity is 30,000 Lux, main wavelength 365 nm). After irradiated, the PAN film was immersed in acetone solution at least 5 h and ultrasonic cleaning 10 min to remove unmodified BP and ITX. Finally, the films was dried in an oven at 30 °C for at least 12 h and stored in a dark place, completed the first modification step. UV–vis (UV-3600, Shimadzu Corporation, Japan) measurements were used to check the modified result of BP and ITX onto PAN surface. Before the measurements, the films were cut and fixed on specimen stages.

BA and PEGDA were purified by passing through a basic alumina column before use. The monomers were formulated into 80 wt% acetone solutions in 10 mL sample bottles according to different ratios and denoted as Px (x = 0, 25, 50, 75 and 100, meaning mole percent of BA monomers). The second step of the grafting process is similar to the first step of modification. A typical synthesis procedure of P$_{50}$ coatings was as

follows: First, the modified PAN film was placed on a quartz plate, and then 100 μL of the P$_{50}$ solution was gently pressed on the surface of the film with a quartz plate to form a thin liquid layer and discharge bubbles. Finally, the model was placed under a high-pressure mercury lamp and irradiated at room temperature for 8 min to complete the grafting process. The grafted films were immersed in dichloromethane and ethanol in sequence, soaked for 12 h and ultrasonically cleaned for 30 min each time to remove unreacted monomers and homopolymers. The surfaces of the films were washed with ethanol and dried in vacuum to constant weight to obtain PAN films with graft coatings. All the solutions involved in the above process were deoxygenated with bubbling nitrogen for 20 min before use.

The conversion and grafting degree of the monomer were confirmed by weighing the film quality and calculated by the following formulas:

$$\text{Monomer Conversion} = (W_1 - W_0)/W_2 \times 100\% \tag{1}$$

$$\text{Grafting Degree} = (G_1 - G_0)/G_0 \times 100\% \tag{2}$$

Here, W_0 and G_0 respectively represent the total and the per unit area quality of the blank film (10 mm diameter disc sample). W_1 and G_1 respectively represent the total and the per unit area quality after photografting. W_2 represents the total quality of monomers added to the surface of the film.

The coatings were characterized with Attenuated Total Reflection Fourier Transform Infrared Spectroscopy (ATR-FTIR), Energy Dispersive Spectrometer (EDS), water Contact Angle (WCA), Scanning Electron Microscope (SEM) and Atomic Force Microscope (AFM). ATR-FTIR was performed on Spectrum 100 spectrometer (PerkinElmer Co. Ltd., USA). CA was performed on a JC2000C (Zhongchen digital technic apparatus Co. Ltd., China). The image of 2 μL of water droplets on the sample is recorded by a digital video camera. For each group, take at least three measurements for calculating average values. AFM images of films were obtained by Dimension Fastscan 2 (Bruker Co. Ltd., Germany). EDS and SEM measurement were obtained using JSM-7500F (JEOL Ltd., Japan). Spray gold on the sample before measurement and set the voltage at 10.0 kV.

2.4. Resistance to fungal adhesion tests

A typical mold *A. niger* was used in this study. The stored *A. niger* was transferred from the slant culture medium to the wort agar medium with a transfer loop, and cultured in a mold incubator at 30 °C for 7 days. After that the spores on the surface of the culture medium were scraped with transfer loop and transferred to a Cryogenic Vials with 20% (*v*/v) glycerin physiological saline solution to obtain spore solution.

To evaluate the fungal repelling activity of different coatings, all samples with graft coating were cut into circles with a diameter of 10 mm, and the blank PAN film was used as a control.

The "landing experiment" was performed to study the interaction of *A. niger* and different coatings. In short, each side of five samples with
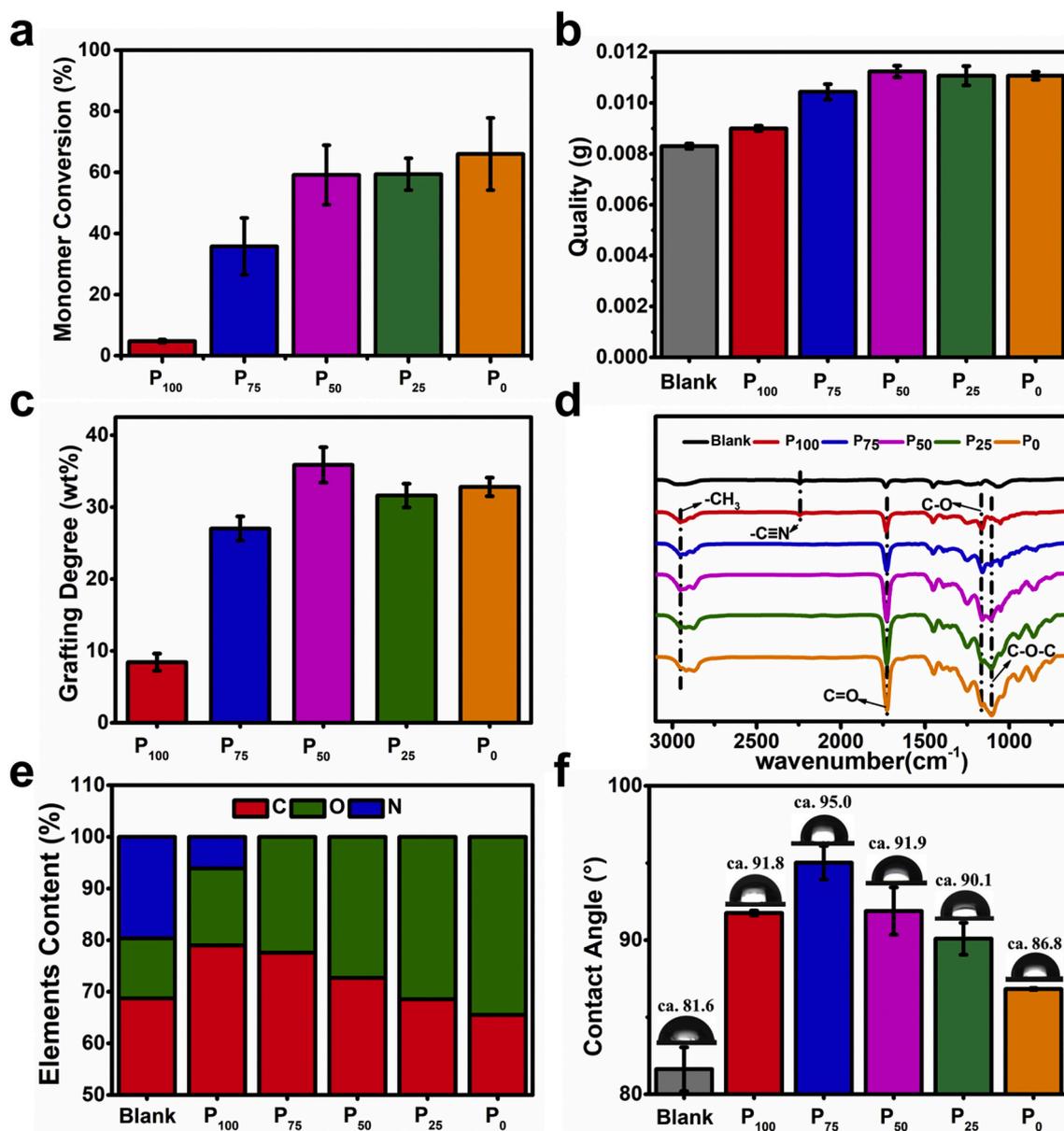
Fig. 1. The net mass change and structure characterization of surface photografting with different coating rates. (a) Monomer conversion, (b) net mass, (c) grafting degree, (d) ATR-FTIR Spectrum (e) EDS, and (f) water contact angle.

different coatings and blank sample were under a UV lamp. The coated side was fixed upward on the surface of the wort agar medium. Then, 7 μL of the spore solution was dripped on the medium about 15 mm from the sample for forming the culture model. Finally, the model was placed in 30 °C mold incubator, and photographs were taken every 24 h to observe the film surface contamination by *A. niger*. Each experiment was repeated at least three times.

3. Results and discussion

3.1. Coating characterization

Since the two photoinitiators have ultraviolet absorption characteristics [29,30], UV–vis was used to prove whether the photoinitiator was successfully grafted onto the substrate in the first step [31] (Fig. S1). As previous study [28], the second step graft polymerization of acrylic monomers can be initiated when the absorbance of the modified substrate by the initiator reaches 0.08 at about 385 nm. Compared with the

blank sample, sufficiently strong absorption band at 265 nm and 385 nm can be observed in the modified film, these absorption bands were believed to be related to the uniform modification of BP and ITX.

Then, net mass change was calculated to check the monomer conversion and grafting degree. Fig. 1a shows the monomer conversion of different coatings. The P_{100} coating has low monomer conversion, only 4.8% according to formula (1). The monomer conversion rate of the P_{75} coating improves to 35.8%. When the PEGDA content reaches 50%, 75%, and 100%, the monomer conversion rates are 59.2%, 59.4%, and 66.0%, respectively. Fig. 1b shows the net mass of different samples per unit area (10 mm diameter disc sample). Compared with the blank group, the mass increase of P_{100}, P_{75}, P_{50}, P_{25}, and P_0 are 0.7 mg, 2.13 mg, 2.93 mg, 2.77 mg, and 2.77 mg respectively. Thus, the grafting degrees (Fig. 1c) are 8.4%, 27.0%, 35.9%, 31.6%, and 32.8% respectively, according to formula (2). This fact is roughly consistent with the measurement of the above monomer conversion results. P_{100} has the lowest grafting degree. The grafting degree of P_{75} is improved when adding a small amount of PEGDA. Further increasing the addition
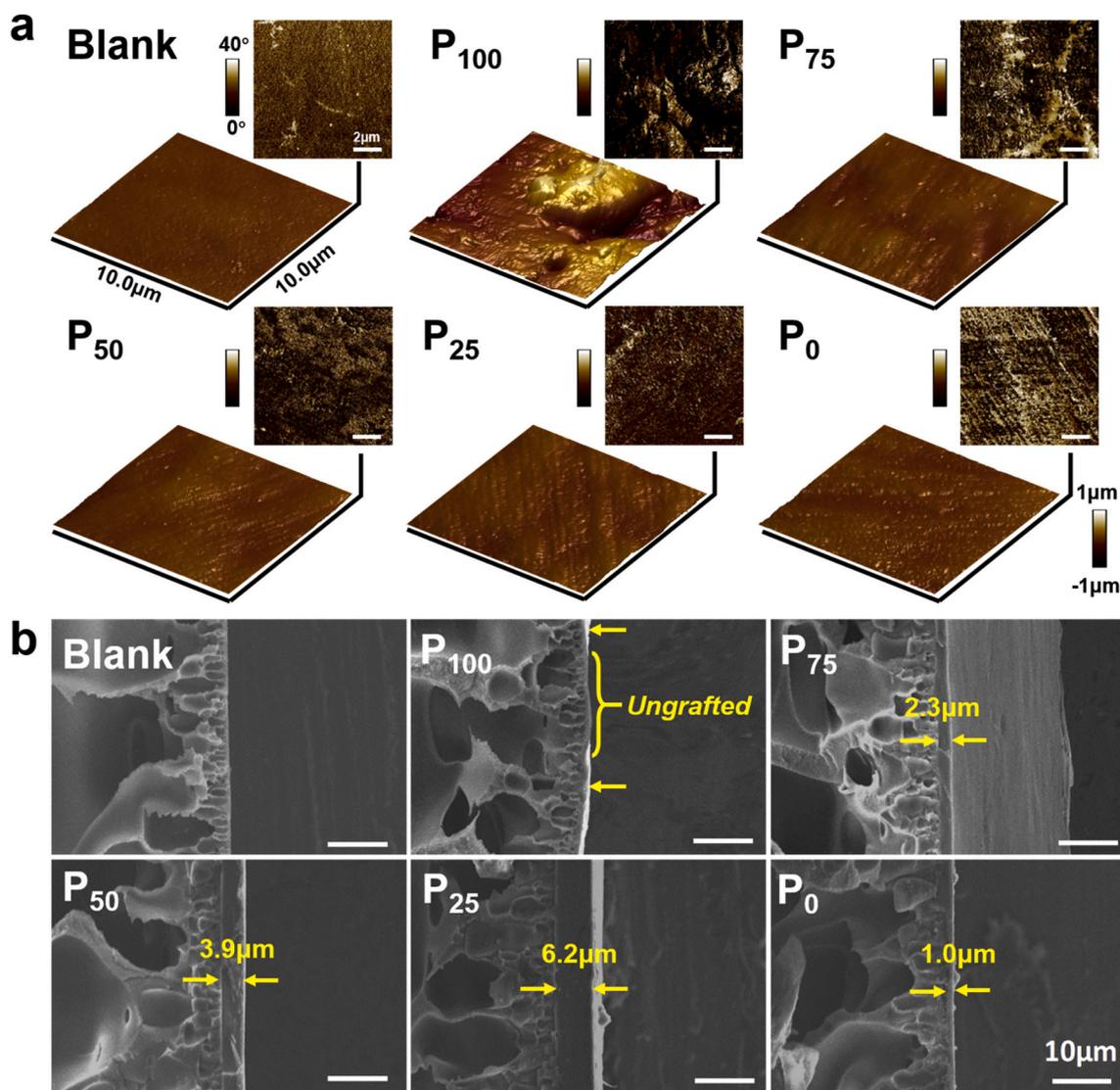
Fig. 2. Surface morphology of the coatings. AFM surface height and phase images (a), and SEM cross-section images (b) of blank, P_{100}, P_{75}, P_{50}, P_{25} and P_0 samples.

amount of PEGDA, the grafting degrees are up to 30%. P_{50} has the highest grafting degree, but there is no statistical difference from the other two samples (P_{25}, P_0). Together, these results suggest that BA monomer caused insignificant net mass changes, which may be due to the large carbon cage of the BA monomer that leads to an increase in steric hindrance and reduces collisions with surface free radicals. However, with the addition of PEGDA, the monomer conversion has been greatly improved. PEGDA increases the probability of collision with the surface free radicals; moreover, PEGDA with bifunctional groups can form a stable coating with a crosslinked structure. These results indicated that the addition of PEGDA improved the stability of the grafted coating since the mass change tended to be constant.

The purpose of ATR-FTIR characterization was to determine the functional groups and chemical bond types of different coatings. (Fig. 1d). A significant –CH_3 stretching absorption peak at 2959 cm^{-1} was found in all grafted samples, which is unique to methyl groups of borneol molecules. In addition, all grafted samples showed characteristic peaks of polyacrylate at 1720 cm^{-1} for C=O and 1160 cm^{-1} for C—O. Meanwhile, compared with the peaks of the P_{100} sample, the P_0, P_{25}, P_{50}, P_{75} samples appeared a new peak at 1100 cm^{-1}, corresponding to the signal of C—O—C stretching, which is the characteristic peak of polyethylene glycol. It is worth noting that as the proportion of monomers changes, the characteristic peaks corresponding to the two

monomers show regular changes. As expected, the two monomers were successfully grafted to the PAN surface in the corresponding proportion. However, the characteristic peak of –C ≡ N (2240 cm^{-1}), which is unique to the PAN substrates, was detected in the blank and group P_{100} but not in P_0, P_{25}, P_{50}, P_{75}. Therefore, it implied that the graft coating of P_{100} has not been completely covered with grafting polymer, while the graft coating of P_0, P_{25}, P_{50}, P_{75} had a continuous coverage.

EDS was used to measure the C, O, N elemental composition of the coatings and the control group. Fig. 1e shows that with the increase content of PEGDA monomer, the percentage of O element has a regular upward trend, which is because the PEGDA monomer contains more O atoms than BA monomer. Similarly, the N element in the P_{100} group further proves that the PBA-grafted coating is a discontinuous coverage. This is consistent with ATR-FTIR result.

The water CA (WCA) was used to exhibit the wettability of the coatings. Fig. 1f shows the blank group a hydrophilic WCA of 81.6°. In the sequence from P_{100} to P_0, the WCA exhibits an enhancement of hydrophobicity in the order of 91.8°, 95.0°, 91.9°, 90.1° and 86.8°, respectively. This phenomenon can be attributed to an increase in the content of PEGDA units on the surface. Since BA units have a large hydrophobic carbon cage structure, while the PEG unit is hydrophilic, when PEGDA units increased in the coating, the hydrophilic properties should gradually improve. But, an interesting phenomenon is that the
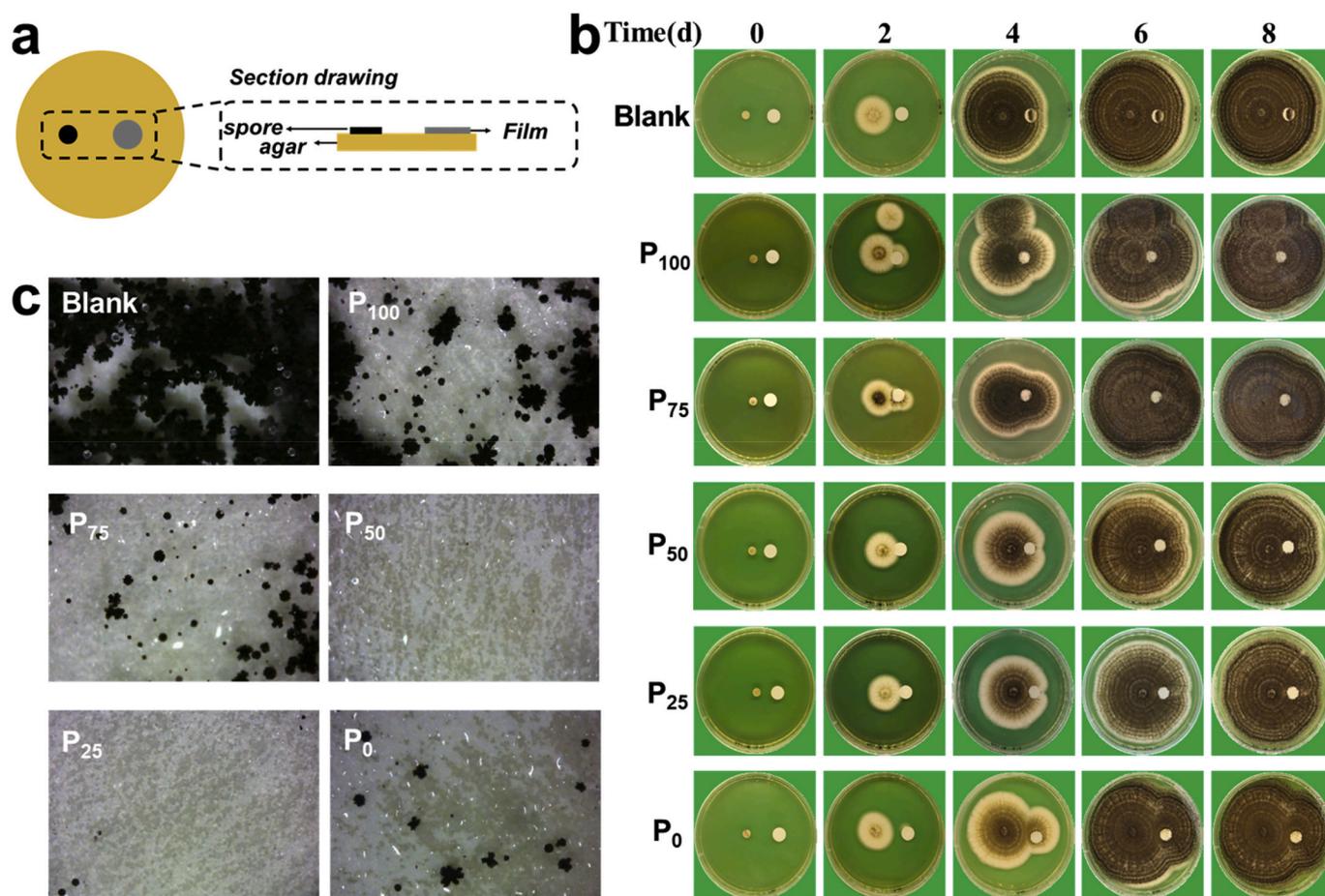
Fig. 3. (a) Schematic illustration of "Landing experiment" experiment for *A.niger* repelling assay of coatings. Contamination of surfaces of different materials (b) and their micrographs (c).

surface of P$_{75}$ showed higher hydrophobic WCA than P$_{100}$. On one hand, the poor modified quality of P$_{100}$ could not completely cover the PAN substrate. The exposure of the PAN substrate results in a relatively lower hydrophobicity. On the other hand, the addition of PEGDA increases the grafting degrees of P$_{75}$ (from 8.4% to 27.0%). In another word, far more BA units are grafted to the surface of the group P$_{75}$. Thus, P$_{75}$ exhibits the highest hydrophobicity among all groups.

In order to confirm the structural morphology of coating, the samples were characterized by AFM and SEM. The height and phase images of these surfaces were obtained via AFM (Fig. 2a). The AFM height images showed the surface roughness. In the sequence from P$_{100}$ to P$_0$, the roughness Rq were 201, 46.1, 40.3, 45.2, and 36.8 nm, respectively. The Rq of the blank sample was 23.5 nm. P$_{100}$ group has a relatively higher roughness, while there is no significant difference in roughness and surface morphology of the group to which the PEGDA was added. The corresponding phase images further provide more information of the surface structure. Compared with the blank group, all coatings appeared microphase separation phenomenon. Due to the exposure of the substrate, P$_{100}$ can observe larger separation domains. However, P$_0$ also has separation domain, which may be due to the formation of hydrophilic polyethylene glycol segments and hydrophobic polyester segments. It is worth noting that after the two monomers are grafted onto the surface of the substrate, slight microphase separation structure was appeared in P$_{25}$ and P$_{50}$, while large size separation domains were observed in the P$_{75}$ group. Thus the ratio of BA/PEGDA in the coating played an important role in the appearance of microphase separation. When the ratio of BA/PEGDA was 1/1 or 1/3, the two polymers in the coating are uniformly dispersed. With the gradual increase of BA addition, the two polymers cannot be well dispersed. When pure BA is grafted on the

surface, the continuous phase structure cannot be formed. This is because pure BA has low grafting efficiency. BA is grafted onto the surface of the substrate in the form of a polymer island, meanwhile a large number of polymers exist as homopolymers without being grafted on the surface. Similarly, it can be seen from the SEM (Fig. S2) results that the coatings of P$_{75}$, P$_{50}$, P$_{25}$ and P$_0$ have relatively smooth structures, while the surface of the group of P$_{100}$ is uneven. Fig. 2b shows the cross-section SEM images of different coatings. Compared with the blank group, all samples containing PEGDA monomer can clearly see the uniform and continuous graft coatings. However, ungrafted substrate was observed in the P$_{100}$ group. This is consistent with the structure of the discontinuous phase grafted by the pure BA we previously speculated.

3.2. Resistance to fungal adhesion

The resistance to fungal adhesion of different coatings against *A. niger* was investigated, as shown in Fig. 3. A visual "landing experiment" model (Fig. 3a) is designed. Briefly, samples with different coatings were co-cultured with *A. niger*, and recorded the contamination of the material surface at regular intervals. Fig. 3b shows the inhibition results of *A. niger* landing. By the fourth day, the surface of the blank group had been contaminated with *A. niger* and a large number of spores were adhered. P$_{100}$, P$_{75}$ and P$_0$ showed different degrees of spore adhesion on their surface. In the P$_{25}$ and P$_{50}$ groups, spores were found only at the edges and most of the surfaces were clean enough. After 8 days, the spore adhesion on the blank, P$_{100}$, P$_{75}$ and P$_0$ surface was aggravated, but the surfaces of the P$_{25}$ and P$_{50}$ groups were still clean besides the edges. A microscope was used to more accurately observe the
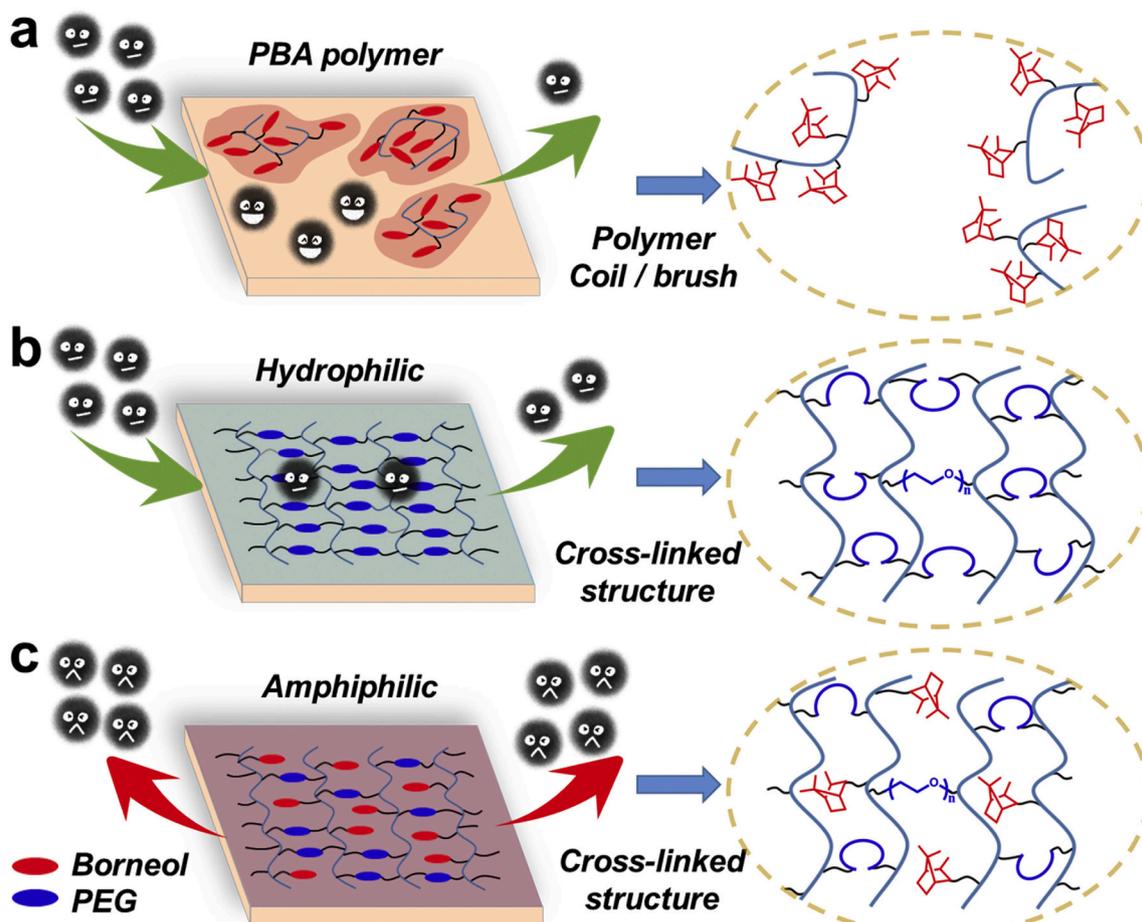
Scheme 2. Schematic representation of the fungal repelling mechanism of P_{100} (a) P_0 (b) and P_{50} (c) coatings.

adhesion of spores on the surface after 8 days. As shown in Fig. 3c, spores adhesion were seen on the central of the surface of blank, P_{100}, P_{75} and P_0, and sporadic spores were also observed on the surface of the P_{25} coating; while no spores adhesion was found on the surface of the P_{50} coating. From the previous characterization, the P_{50} and P_{25} coatings have a more uniform continuous phase structure, which can effectively prevent the adhesion of *A. niger*. An emergent phenomenon is that the coatings of P_{100} and P_0 cannot completely resist spore adhesion; when equivalent PEGDA and BA are added (Fig. 3c, P_{50}), the anti-adhesion effect is the best. These results indicated that BA and PEGDA have a synergistic effect against the adhesion of *A niger*.

3.3. Fungal repelling mechanism

As a filamentous fungus, *A. niger* can grow from any spore and contaminate many substrates. Due to the stereochemical structure, borneol cage has been shown to have anti-adhesion properties when it was grafted on substrates [14,16]. However, limited by reaction efficiency of the BA monomer, the island pattern of the P_{100} coating will cause the exposure of the hydrophilic substrate, thus cannot resist the adhesion of *A. niger* (Scheme 2a). In contrast, the P_0 coating can effectively form a continuous grafted coating structure, but because of its hydrophilicity (Scheme 2b), it provides a suitable wet surface for *A. niger*, and even the unique glycol coil stereochemical structure is not enough to completely inhibit *A. niger* adhesion. However, the copolymer coating formed by BA and PEGDA is a hydrophilic/hydrophobic combination, and this strategy has been considered to be effective in the field of microbe repelling [32–34]. Our work indicated the coating formed by borneol cage and glycol coils possesses the continuous coating. The

unique amphiphilic stereochemical coating (Scheme 2c) can effectively prevent the fungal active adhesion on its surface.

4. Conclusion

The starting point of this study was to build a uniform and stable fungal repelling coating with stereochemical strategy by surface photografting. We first tried to graft the monomer BA onto the surface of substrate, but the fungal repelling effect was not good due to the poor grafting ratio. PEGDA has the good grafting ratio, but the hydrophilic surface showed unsatisfied anti-adhesion property. From the perspective of binary cooperation, PEGDA was introduced as another functional monomer to synthesize a composite coating with BA. Under the modulated ratios of the bi-molecules, high quality continuous coatings can be realized. They all show a certain resistance to fungal adhesion, but when the ratio of the two monomers is 1:1, the anti-adhesion effect is the best, which is not available when each monomer is used alone. This case provided a deeper insight into the area of fungal repelling strategy based on surface stereochemistry. That is, for the first time, the combination of stereochemical bi-molecules, borneol (with a cage molecular structure) and glycol (with a coil molecular structure), has proven to be efficient and simple to form an amphiphilic coating by surface photografting with powerful fungal repelling performance. Based on the understanding of this amphiphilic stereochemical antimicrobial strategy it is promising to design and develop new microbial anti-adhesion materials and surfaces for the wide biomedicine and biosafty applications.

Author Statement

The corresponding author X. Wang is responsible that the descriptions are accurate and agreed by all authors. C. Chen designed the experiments and carried out materials preparation and evaluation, data analysis, writing-original draft. Z. Xie conducted data analysis and mechanism discussion. P. Zhang performed evaluation and data analysis of physical and chemical properties of the coatings. Y. Liu assisted in evaluating of materials and refining the draft. X. Wang conceived and designed the research plan, refined the draft, supervised the project and contributed to the funding acquisition. All the authors contributed to the interpretation of the results and data analysis and edited the manuscript at all stages.

Declaration of Competing Interest

The authors declared that there is no conflict of interest.

Acknowledgments

Appendix A. Supplementary data

Supplementary data to this article can be found online at https://doi.org/10.1016/j.colcom.2020.100336.

References

[1] C.R. Arciola, D. Campoccia, P. Speziale, L. Montanaro, J.W. Costerton, Biofilm formation in Staphylococcus implant infections. A review of molecular mechanisms and implications for biofilm-resistant materials, Biomaterials 33 (2012) 5967–5982, https://doi.org/10.1016/j.biomaterials.2012.05.031.

[2] C.G. Otoni, P.J.P. Espitia, R.J. Avena-Bustillos, T.H. McHugh, Trends in antimicrobial food packaging systems: emitting sachets and absorbent pads, Food Res. Int. 83 (2016) 60–73, https://doi.org/10.1016/j.foodres.2016.02.018.

[3] D. Campoccia, L. Montanaro, C.R. Arciola, A review of the biomaterials technologies for infection-resistant surfaces, Biomaterials 34 (2013) 8533–8554, https://doi.org/10.1016/j.biomaterials.2013.07.089.

[4] X. Ding, S. Duan, X. Ding, R. Liu, F.-J. Xu, Versatile antibacterial materials: an emerging arsenal for combatting bacterial pathogens, Adv. Funct. Mater. 28 (2018), https://doi.org/10.1002/adfm.201802140.

[5] T. Wei, Q. Yu, H. Chen, Responsive and synergistic antibacterial coatings: fighting against bacteria in a smart and effective way, Adv. Healthc. Mater. 8 (2019), e1801381, https://doi.org/10.1002/adhm.201801381.

[6] H. Ren, Y. Du, Y. Su, Y. Guo, Z. Zhu, A. Dong, A review on recent achievements and current challenges in antibacterial electrospun n-halamines, Colloid Interface. Sci. Commun. 24 (2018) 24–34, https://doi.org/10.1016/j.colcom.2018.03.004.

[7] J. Buxadera-Palomero, C. Calvo, S. Torrent-Camarero, F.J. Gil, C. Mas-Moruno, C. Canal, D. Rodriguez, Biofunctional polyethylene glycol coatings on titanium: an in vitro-based comparison of functionalization methods, Colloid Surf. B-Biointerfaces 152 (2017) 367–375, https://doi.org/10.1016/j.colsurfb.2017.01.042.

[8] S. Chen, L. Yuan, Q. Li, J. Li, X. Zhu, Y. Jiang, O. Sha, X. Yang, J.H. Xin, J. Wang, F. J. Stadler, P. Huang, Durable antibacterial and nonfouling cotton textiles with enhanced comfort via zwitterionic sulfopropylbetaine coating, Small 12 (2016) 3516–3521, https://doi.org/10.1002/smll.201600587.

[9] P. Kaali, E. Strömberg, R.E. Aune, G. Czél, D. Momcilovic, S. Karlsson, Antimicrobial properties of ag+ loaded zeolite polyester polyurethane and silicone rubber and long-term properties after exposure to in-vitro ageing, Polym. Degrad. Stabil. 95 (2010) 1456–1465, https://doi.org/10.1016/j.polymdegradstab.2010.06.024.

[10] A. Rai, A. Prabhune, C.C. Perry, Antibiotic mediated synthesis of gold nanoparticles with potent antimicrobial activity and their application in antimicrobial coatings, J. Mater. Chem. 20 (2010), https://doi.org/10.1039/c0jm00817f.

[11] C. Alberti, A. Bouakline, P. Ribaud, C. Lacroix, P. Rousselot, T. Leblanc, F. Derouin, G. Aspergillus Study, Relationship between environmental fungal contamination and the incidence of invasive aspergillosis in haematology patients, J. Hosp. Infect. 48 (2001) 198–206, https://doi.org/10.1053/jhin.2001.0998.

[12] L. Luo, G. Li, D. Luan, Q. Yuan, Y. Wei, X. Wang, Antibacterial adhesion of borneol-based polymer via surface chiral stereochemistry, ACS Appl. Mater. Interfaces 6 (2014) 19371–19377, https://doi.org/10.1021/am505481q.

[13] X. Sun, Z. Qian, L. Luo, Q. Yuan, X. Guo, L. Tao, Y. Wei, X. Wang, Antibacterial adhesion of poly(methyl methacrylate) modified by borneol acrylate, ACS Appl. Mater. Interfaces 8 (2016) 28522–28528, https://doi.org/10.1021/acsami.6b10498.

[14] B. Shi, D. Luan, S. Wang, L. Zhao, L. Tao, Q. Yuan, X. Wang, Borneol-grafted cellulose for antifungal adhesion and fungal growth inhibition, RSC Adv. 5 (2015) 51947–51952, https://doi.org/10.1039/c5ra07894f.

[15] G. Li, H. Zhao, J. Hong, K. Quan, Q. Yuan, X. Wang, Antifungal graphene oxide-borneol composite, Colloid Surf. B-Biointerfaces 160 (2017) 220–227, https://doi.org/10.1016/j.colsurfb.2017.09.023.

[16] J. Xu, H. Zhao, Z. Xie, S. Ruppel, X. Zhou, S. Chen, J.F. Liang, X. Wang, Stereochemical strategy advances microbially antiadhesive cotton textile in safeguarding skin flora, Adv. Healthc. Mater. 8 (2019), e1900232, https://doi.org/10.1002/adhm.201900232.

[17] B. Rånby, Surface modification and lamination of polymers by photografting, Int. J. Adhes. Adhes. 19 (1999) 337–343, https://doi.org/10.1016/S0143-7496(98)00066-9.

[18] S. Yuan, J. Zhao, S. Luan, S. Yan, W. Zheng, J. Yin, Nuclease-functionalized poly (styrene-b-isobutylene-b-styrene) surface with anti-infection and tissue integration bifunctions, ACS Appl. Mater. Interfaces 6 (2014) 18078–18086, https://doi.org/10.1021/am504955g.

[19] I. Roppolo, A. Chiappone, K. Bejtka, E. Celasco, A. Chiodoni, F. Giorgis, M. Sangermano, S. Porro, A powerful tool for graphene functionalization: benzophenone mediated UV-grafting, Carbon 77 (2014) 226–235, https://doi.org/10.1016/j.carbon.2014.05.025.

[20] G.M. Harbers, K. Emoto, C. Greef, S.W. Metzger, H.N. Woodward, J.J. Mascali, D. W. Grainger, M.J. Lochhead, Functionalized poly(ethylene glycol)-based bioassay surface chemistry that facilitates bio-immobilization and inhibits nonspecific protein, bacterial, and mammalian cell adhesion, Chem. Mater. 19 (2015) 4405–4414, https://doi.org/10.1021/cm070509u.

[21] X. Ding, C. Yang, T.P. Lim, L.Y. Hsu, A.C. Engler, J.L. Hedrick, Y.Y. Yang, Antibacterial and antifouling catheter coatings using surface grafted PEG-b-cationic polycarbonate diblock copolymers, Biomaterials 33 (2012) 6593–6603, https://doi.org/10.1016/j.biomaterials.2012.06.001.

[22] Z.X. Voo, M. Khan, Q. Xu, K. Narayanan, B.W.J. Ng, R. Bte Ahmad, J.L. Hedrick, Y. Y. Yang, Antimicrobial coatings against biofilm formation: the unexpected balance between antifouling and bactericidal behavior, Polym. Chem. 7 (2016) 656–668, https://doi.org/10.1039/c5py01718a.

[23] J. Guo, W. Wang, J. Hu, D. Xie, E. Gerhard, M. Nisic, D. Shan, G. Qian, S. Zheng, J. Yang, Synthesis and characterization of anti-bacterial and anti-fungal citrate-based mussel-inspired bioadhesives, Biomaterials 85 (2016) 204–217, https://doi.org/10.1016/j.biomaterials.2016.01.069.

[24] M. Broda, Biological effectiveness of archaeological oak wood treated with methyltrimethoxysilane and PEG against Brown-rot fungi and moulds, Int. Biodeterior. Biodegrad. 134 (2018) 110–116, https://doi.org/10.1016/j.ibiod.2018.09.001.

[25] Y. He, G. Chen, Q. Luo, P. Ge, Evaluation of mould growth on wall surface in South China, Procedia Eng. 205 (2017) 4135–4141, https://doi.org/10.1016/j.proeng.2017.10.155.

[26] A. Lugauskas, L. Levinskaitė, D. Pečiulytė, Micromycetes as deterioration agents of polymeric materials, Int. Biodeterior. Biodegrad. 52 (2003) 233–242, https://doi.org/10.1016/s0964-8305(03)00110-0.

[27] C.C. Lai, C.K. Chung, Hydrophilicity and optic property of polyethylene glycol coating on polydimethylsiloxane for fast prototyping and its application to backlight microfluidic chip, Surf. Coat. Tech. 389 (2020), https://doi.org/10.1016/j.surfcoat.2020.125606.

[28] H. Bai, Z. Huang, W. Yang, Visible light-induced living surface grafting polymerization for the potential biological applications, J. Polym. Sci. Pol. Chem. 47 (2009) 6852–6862, https://doi.org/10.1002/pola.23724.

[29] Z. Kecici, G. Temel, Methacrylated benzophenone as triple functional compound for the synthesis of partially crosslinked copolymers, Prog. Org. Coat. 115 (2018) 138–142, https://doi.org/10.1016/j.porgcoat.2017.11.015.

[30] J.-D. Cho, S.-G. Kim, J.-W. Hong, Surface modification of polypropylene sheets by UV-radiation grafting polymerization, J. Appl. Polym. Sci. 99 (2006) 1446–1461, https://doi.org/10.1002/app.22631.

[31] C. Li, A. Glidle, X. Yuan, Z. Hu, E. Pulleine, J. Cooper, W. Yang, H. Yin, Creating "living" polymer surfaces to pattern biomolecules and cells on common plastics, Biomacromolecules 14 (2013) 1278–1286, https://doi.org/10.1021/bm4000597.

[32] F. Qi, Y. Qian, N. Shao, R. Zhou, S. Zhang, Z. Lu, M. Zhou, J. Xie, T. Wei, Q. Yu, R. Liu, Practical preparation of infection-resistant biomedical surfaces from antimicrobial beta-peptide polymers, ACS Appl. Mater. Interfaces 11 (2019) 18907–18913, https://doi.org/10.1021/acsami.9b02915.

[33] U. Dani, A. Bahadur, K. Kuperkar, Micellization, antimicrobial activity and curcumin solubilization in gemini surfactants: influence of spacer and non-polar tail, Colloid Interface. Sci. Commun. 25 (2018) 22–30, https://doi.org/10.1016/j.colcom.2018.06.002.

[34] X.-H. Zhang, H.-X. Wu, L. Huang, C.-J. Liu, From homogeneous to heterogeneous: a simple approach to prepare polymer brush modified surfaces for anti-adhesion of bacteria, Colloid Interface. Sci. Commun. 23 (2018) 21–28, https://doi.org/10.1016/j.colcom.2018.02.002.